PROCEEDINGS OF SCIENCE

Disentangling Cosmic-Ray Transport inside Starburst Nuclei with Gamma-ray and Neutrino Telescopes

A. Ambrosone,[a,b,*] **M. Chianese,**[a,b] **D.F.G. Fiorillo,**[c] **A. Marinelli**[a,b,d] **and G. Miele**[a,b,e]

[a] *Dipartimento di Fisica "Ettore Pancini", Università degli studi di Napoli "Federico II", Complesso Univ. Monte S. Angelo, I-80126 Napoli, Italy*

[b] *INFN - Sezione di Napoli, Complesso Univ. Monte S. Angelo, I-80126 Napoli, Italy*

[c] *Niels Bohr International Academy, Niels Bohr Institute, University of Copenhagen, Copenhagen, Denmark*

[d] *INAF-Osservatorio Astronomico di Capodimonte, Salita Moiariello 16, I-80131 Naples, Italy*

[e] *Scuola Superiore Meridionale, Università degli studi di Napoli "Federico II", Largo San Marcellino 10, 80138 Napoli, Italy*

E-mail: antonio.ambrosone@unina.it

In this contribution, we discuss the signatures of the Cosmic-Rays (CRs) transport inside Starburst nuclei (SBNi) onto gamma-ray and neutrino fluxes. In particular, we quantify the potentiality of future measurements such as CTA and SWGO to distinguish between different scenarios. We also discuss the implications for future opportunities offered by current and upcoming neutrino telescopes.

38th International Cosmic Ray Conference (ICRC2023)
26 July - 3 August, 2023
Nagoya, Japan

*Speaker

PoS(ICRC2023)1486

1. Introduction

Starburst Galaxies are astrophysical sources of great interest. They manifest significant star-forming activity [1]. This means that they can considered as laboratories for many multi-messengers studies. From the observational point of view, they are characterised by a high infrared luminosity [2–4] (which trace the star formation rate), the Auger collaboration has find compelling evidence of a correlation between SBGs with high-energy cosmic-rays [7, 8]. A dozen of these sources have been also detected to be GeV gamma-ray emitters by the Fermi-LAT telescope (see for instance [2]) . Indeed, such GeV luminosity correlates with the infrared luminosity [2–4], reinforcing the idea that star-forming processes are responsible for such emissions. Furthermore, M82 and NGC253 have also been detected as TeV gamma-ray emitters [5, 6]. In this contribution, we investigate how different cosmic-rays transport models impact the gamma-ray and neutrino observations from local SBGs (see [9] for more details). We quantify, using only public information, the potentiality of the Cherenkov Telescope Array (CTA) [10] to detect local SBGs. Furthermore, we discuss the opportunities offered by current and upcoming neutrino telescopes [11, 12]. The proceeding is organized as follows: Sec. 2 describes the CR transport models analyzed, Sec. 3 describe the phenomenological signature on gamma-ray fluxes of the different models. Sec. 4 shows a forecast analysis for the CTA telescope. Sec. 5 shows the implications for the Neutrino Astronomy and Finally, we conclude in Sec. 6.

2. Cosmic-Rays Transport Models

Starburst Galaxies are generally characterised by a central core, usually referred as starburst nucleus (SBN) [13–16]. We model the CR transport inside this region, using a leaky-box model approach (following the approach of Refs. [13, 14], which was also employed by Ref. [15, 16]. Also Ref. [17] has previously used a leaky-box model for SBNi). This is justified by the fact that SBNi are usually small regions ($\sim 200\,\mathrm{pc}$) compared to the entire galaxies and we also do not expect any time variability from these sources (this is also phenomenologically verified since these sources do not show any statistical-relevant time variation in their light curves [2]).

The CR distribution inside can be written as [9]

$$f(p) = Q(p) \cdot \tau_{pp}(p) F_{\mathrm{cal}} \tag{1}$$

where $Q(p)$ is the power-law injected by SNRs. τ_{pp} is proton-proton collision timescale

$$\tau_{\mathrm{pp}}(p) = \frac{1}{k\sigma_{pp}(p) \cdot c \cdot n_{\mathrm{ISM}}} \tag{2}$$

where $k = 0.5$ is the inelasticity of the process and $\sigma_{pp}(p)$ is the inelastic energy-dependent proton-proton cross section [18]. c is the light velocity in vacuum space and finally n_{ISM} is the gas density which is the target for high-energy protons. F_{cal} is the so called calorimetric fraction, which physically represents the fraction (between 0 and 1) of high-energy protons which effectively end up producing gamma-rays and neutrinos. F_{cal} depends on the different CR dynamical timescale. In this contribution, we test two different models for CR transport inside SBNi. The first model is given by Ref. [13, 14] (which has been also employed by Ref. [15, 16]). This model (hereafter model A)

considers diffusion in a strong-turbulence scenario given by an external magnetic field B. Indeed, the diffusion timescale is described by a Kolmogorov-like scenario where the timescale $\tau_{\rm diff} \propto E^{-1/3}$, where it generally provides a very marginal contribution to the CR transport. Indeed, the transport is mainly driven by advection phenomena which are described by an energy-independent timescale $\tau_{\rm adv} = R/v_{\rm wind}$ and finally the energy-losses are dominantly dominated by pp collisions. model A usually provides a energy-independent $F_{\rm cal}$ which result in a gamma-ray (and neutrino) flux following a power-law spectrum with a spectral index $\gamma = \alpha - 2$ where α is the proton spectral index injected $Q(p)$.

On the contrary, model B, developed by Ref. [19] (employed also by Refs. [20, 21]), neglects any advection phenomena (this because from a theoretical point of view, the advection should be driven by ionized gas, but SBGs are expected to be mostly filled by cold gas [19]). Furthermore, the diffusion is not considered to be produced by an external turbulence. Indeed, it is supposed to be driven by the self-turbulence by the alven waves generated by CRs themselves, with a diffusion coefficient proportional to the streaming velocity of CRs [19].

Another difference between model A and model B is given by the different geometries they take into account. In fact, model A consider the nucleus as a compact spherical region, while model B considers it a cylinder. This induces a different form for the calorimetric fractions.

For model A [9]:

$$F_{\rm cal} = \frac{\tau_{\rm eff}}{\tau_{\rm eff} + 1} \tag{3}$$

where $\tau_{eff} = \tau_{esc}/\tau_{pp}$ is the effective optical depth of the SBN. $\tau_{\rm esc}$ is the timescale needed for a CR to escape from the nucleus and it physically depends on the CR model considered.

For model B [9, 19]:

$$F_{\rm cal} = 1 - \left[{}_0F_1\left(\frac{1}{5}, \frac{16}{25}\tau_{\rm eff}\right) + \frac{3\tau_{\rm eff}}{4M_A^3}\, {}_0F_1\left(\frac{9}{5}, \frac{16}{25}\tau_{\rm eff}\right)\right]^{-1} \tag{4}$$

where $M_A \simeq 2$ is the Mach number. The diffusion coefficient, for model B, depends on several parameters and it can be written as [9]

$$\begin{aligned} D \propto V_s = \mathrm{Min}\Bigg[& \mathrm{c}, \mathrm{V_{al}}(1 + 2.3 \cdot 10^{-3} \cdot \left(\frac{\mathrm{E}}{\mathrm{m_p}}\right)^{\alpha-3} \times \\ & \times \left(\frac{n_{\rm ISM}}{10^3}\right)^{3/2} \left(\frac{\chi}{10^{-4}}\right) \left(\frac{\sigma_g}{10\sqrt{2}\,\mathrm{Kms^{-1}}}\right)\Bigg] \end{aligned} \tag{5}$$

where $V_{\rm al}$ is the alven velocity, m_p and E are the proton mass and energy, $\chi \simeq 10^{-4}$ is the assumed ionised fraction (the fraction ionised gas) and σ_g is the dispersion velocity. $\tau_{\rm esc} = \tau_{\rm diff} = h^2/D$, where h is the height of the cylinder.

3. Differences between model A and B onto Gamma-ray Spectrum

In this section, we report the phenomenological signatures of model A and model B in the gamma-ray spectra.

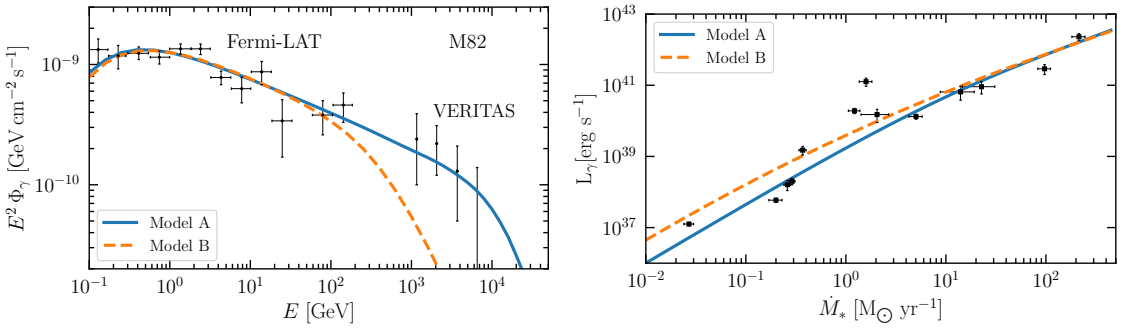

Figure 1: Left: Comparison between the best-fit spectra for M82 for model A (blue) and model B (orange). For reference current data are shown [2, 5] **Right**: Gamma-ray integrated luminosity between [0.1 – 100] GeV for model A (blue) and model B (orange) as a function of the star formation rate. The black data points refer to the local SBG data reported by Ref. [3]. Images taken from Ref. [9]

Fig. 1 shows difference in the gamma-ray spectrum for model A and model B. In particular, on the left, the best-fit values to the current M82 data [2, 5] both for model A and model B are shown. On the right, the integrated between $[0.1 - 100]$ GeV for model A and model B, is shown as a function of the star formation rate. It is compared with the data from local SBG reported by Ref. [3]. Interestingly, model B struggles to accommodate TeV data from the source [9]. In fact, for this model SBG stops being calorimetric for $E_\gamma \geq 100 - 1000\,\mathrm{GeV}$, being dominated by diffusion escape. On the other hand, model A provides a pure power-law spectrum since the CR transport is dominated by time-independent timescales and F is energy-indepedent.

The integrated luminosity is evaluated injecting a $E^{-4.2}$ proton spectrum for both models [9]. We notice that for $\dot{M}_* \lesssim 10\,\mathrm{M}_\odot\,\mathrm{yr}^{-1}$, the luminosity of model B is higher than the luminosity of model A. This is due to the different geometry considered by the two models. By contrast, for higher SFR the luminosity is same because the SBGs start being totally calorimetric. These examples show that the major difference between model A and model B stands for the TeV data. In the following section, we show the results from a forecast from the Cherenkov Telescope Array (CTA) [10].

4. Simulated Data for CTA

In the previous section, we argued that the biggest difference between model A and model B reside in the TeV gamma-ray data. Therefore, here, we report the results of a forecast (for the CTA telescope [10]) we performed over starburst nuclei (In this proceeding we report results for M82 and NGC253). Since model A provides higher fluxes at higher energies, it consequently provides better expectations for CTA. Under the hypothesis of model A being true, we generate 10^4 pseudo mock data sets for the CTA telescope and we quantify the statistical confidence to reject model B (see [9] for the full treatment).

We consider the energy bins where the expected flux are above the sensitivity. Then, we evaluate the expected number of signal events through [9]:

$$n_s = T_o \int_{\Delta E} A_{\mathrm{eff}}(E)\phi_s(E)dE \tag{6}$$

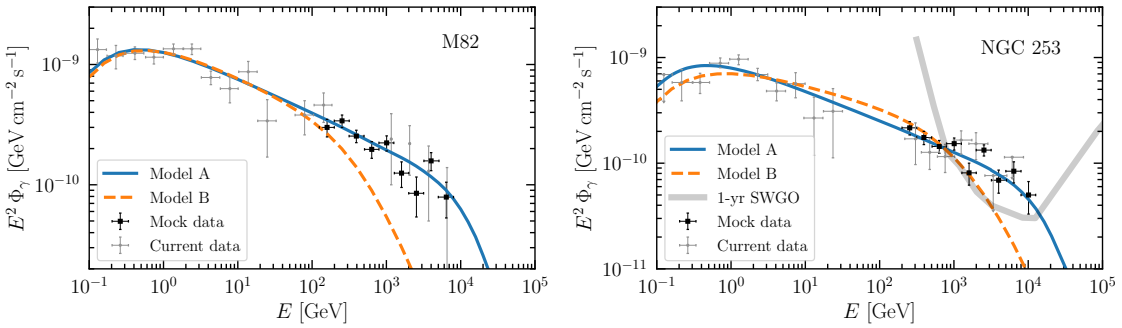

Figure 2: Left: mock dataset for M82 (black data points) compared with model A and current data [2, 5] (grey data points). We also impose model B. **Right**: Mock dataset for NGC 253 (black data points), compared with current data [2, 6] (grey data) and with model A and model B. We also impose the expected SWGO sensitivity [22, 23]. Images taken from Ref. [9].

T_o is the observation time, which we consider to be 50 h. $A_{\rm eff}(E)$ is the energy-dependent effective area after the cuts are applied [10]. $\phi_s(E)$ is the signal flux according to model A. The expected number of background events, by the public expected background rate per unit of solid angle [10]. We multiply it by T_o and by Max$[\Delta\Omega_{\rm SBN}, \Delta\Omega_{\rm res}]$, namely by the minimum between the intrinsic dimension of the SBN and the expected energy-dependent energy resolution of the experiment [9, 10]. We randomly generate 10^4 numbers according to a poisson distribution with a mean number $\mu = n_s + n_{\rm back}$. We determine the empirical number of measured signal events by evaluating $\tilde{n}_s = n_{\rm gen} - n_{\rm back}$. The extracted spectral energy distribution (SED) is then evaluated as [9]

$$\mathrm{SED_i} = \frac{\tilde{\mathrm{n}}_\mathrm{i}}{\mathrm{T_o}\int_{\Delta\mathrm{E}} \mathrm{A_{eff}(E)}\left(\frac{\mathrm{E}}{1\,\mathrm{GeV}}\right)^{-2}\mathrm{dE}} \tag{7}$$

Eq. 7 assumes that the spectrum is a E^{-2} in each bin, but since the dimension of the bin is small, this assumption has not impact in the final result.

Fig. 2 shows a mock SED data both for M82 and NGC253 (black data points). We also compare the best-fit for model A and model B. For NGC253, we also show the SWGO expected sensitivity [22, 23]. This future telescope will also probe the emission of this source. We have also evaluated the statistical confidence with which model B can be excluded considering the p-value and the Bayes factor. We obtain that model B will be excluded at more than 2σ C.L. [9].

5. Implications for Neutrino Astronomy

In this section, we discuss the implications for the Neutrino Astronomy for the CR transport inside SBNi. In particular, different CR transport inside SBNi might imply a different contribution with respect to ICeCube diffuse neutrino data. Indeed, if at high energies SBN stop being calorimetric, it means that neutrinos cannot be emitted since CRs start escaping the source. By contrast, if SBNi are calorimetric or dominated by energy-independent, TeV neutrino can be emitted explaining a portion of the IceCube diffuse neutrino data. Fig. 3 shows the diffuse gamma-ray and neutrino contribution for model A (see [9] for further details). The fluxes can explain a big part of the Isotropic gamma-ray background flux (IGRB) measured by Fermi-LAT [24] and also produce

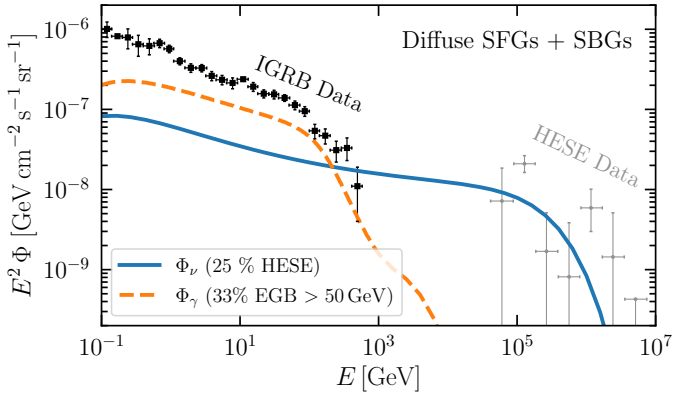

Figure 3: Model A diffuse gamma-ray (orange line) and neutrino (blue line) diffuse fluxes. They are compared with the Fermi-LAR IGRB data [24] and the 7.5 yr HESE data [12]. Imagen taken from Ref. **??**.

$\sim$ 20% of the HESE events registered by the IceCube collaboration [12] (HESE data are also shown in the figure).

6. Conclusions

In this proceeding, we have studied how extra galactic gamma-ray data can be used to discriminate different CR transport models inside SBNi. We have found that current data slightly prefer time-independent CR timescale (as already pointed out by previous publications). We have also produced mock data sets for the Cherenkov Telescope Array and showing that it will unequivocally distinguish between differet transport models. Also other future telescopes are expected to probe the emission of local SBGs, such as SWGO and Astri-mini Array [22, 23, 25]. Further measurements will provide a clear understanding of the non-thermal emissions of SBGs. We have also argued how crucial this will be for neutrino astronomy and in particular for unveiling the origin of the extragalactic HESE spectrum. Finally, we also comment that upcoming neutrino telescopes such as KM3NeT [11, 26] are also expected to probe neutrino emission from local SBGs [27–30] (as pointed out by Ref. [16]), proving that these sources are definitely neutrino emitters.

References

[1] T. A. Thompson, E. Quataert, E. Waxman, N. Murray and C. L. Martin, Astrophys. J. **645** (2006), 186-198 doi:10.1086/504035 [arXiv:astro-ph/0601626 [astro-ph]].

[2] M. Ajello, M. Di Mauro, V. S. Paliya and S. Garrappa, Astrophys. J. **894** (2020) no.2, 88 doi:10.3847/1538-4357/ab86a6 [arXiv:2003.05493 [astro-ph.GA]].

[3] P. Kornecki, L. J. Pellizza, S. del Palacio, A. L. Müller, J. F. Albacete-Colombo and G. E. Romero, Astron. Astrophys. **641**, A147 (2020) doi:10.1051/0004-6361/202038428 [arXiv:2007.07430 [astro-ph.HE]].

[4] P. Kornecki, E. Peretti, S. del Palacio, P. Benaglia and L. J. Pellizza, Astron. Astrophys. **657**, A49 (2022) doi:10.1051/0004-6361/202141295 [arXiv:2107.00823 [astro-ph.HE]].

[5] 2009Natur.462..770V VERITAS Collaboration and 92 colleagues 2009. A connection between star formation activity and cosmic rays in the starburst galaxy M82. Nature 462, 770–772. doi:10.1038/nature08557

[6] H. Abdalla *et al.* [H.E.S.S.], Astron. Astrophys. **617** (2018), A73 doi:10.1051/0004-6361/201833202 [arXiv:1806.03866 [astro-ph.HE]].

[7] A. Abdul Halim *et al.* [Pierre Auger], 'Constraining the sources of ultra-high-energy cosmic rays across and above the ankle with the spectrum and composition data measured at the Pierre Auger Observatory," [arXiv:2211.02857 [astro-ph.HE]].

[8] P. Abreu *et al.* [Pierre Auger], Astrophys. J. **935**, no.2, 170 (2022) doi:10.3847/1538-4357/ac7d4e [arXiv:2206.13492 [astro-ph.HE]].

[9] A. Ambrosone, M. Chianese, D. F. G. Fiorillo, A. Marinelli and G. Miele, Mon. Not. Roy. Astron. Soc. **515** (2022) no.4, 5389-5399 doi:10.1093/mnras/stac2133 [arXiv:2203.03642 [astro-ph.HE]].

[10] B. S. Acharya *et al.* [CTA Consortium], WSP, 2018, ISBN 978-981-327-008-4 doi:10.1142/10986 [arXiv:1709.07997 [astro-ph.IM]].

[11] S. Adrian-Martinez *et al.* [KM3Net], J. Phys. G **43**, no.8, 084001 (2016) doi:10.1088/0954-3899/43/8/084001 [arXiv:1601.07459 [astro-ph.IM]].

[12] R. Abbasi *et al.* [IceCube], Phys. Rev. D **104**, 022002 (2021) doi:10.1103/PhysRevD.104.022002 [arXiv:2011.03545 [astro-ph.HE]].

[13] E. Peretti, P. Blasi, F. Aharonian and G. Morlino, Mon. Not. Roy. Astron. Soc. **487** (2019) no.1, 168-180 doi:10.1093/mnras/stz1161 [arXiv:1812.01996 [astro-ph.HE]].

[14] E. Peretti, P. Blasi, F. Aharonian, G. Morlino and P. Cristofari, Mon. Not. Roy. Astron. Soc. **493** (2020) no.4, 5880-5891 doi:10.1093/mnras/staa698 [arXiv:1911.06163 [astro-ph.HE]].

[15] A. Ambrosone, M. Chianese, D. F. G. Fiorillo, A. Marinelli, G. Miele and O. Pisanti, Mon. Not. Roy. Astron. Soc. **503** (2021) no.3, 4032-4049 doi:10.1093/mnras/stab659 [arXiv:2011.02483 [astro-ph.HE]].

[16] A. Ambrosone, M. Chianese, D. F. G. Fiorillo, A. Marinelli and G. Miele, Astrophys. J. Lett. **919** (2021) no.2, L32 doi:10.3847/2041-8213/ac25ff [arXiv:2106.13248 [astro-ph.HE]].

[17] B. C. Lacki and R. Beck, Mon. Not. Roy. Astron. Soc. **430**, 3171 (2013) doi:10.1093/mnras/stt122 [arXiv:1301.5391 [astro-ph.CO]].

[18] S. R. Kelner, F. A. Aharonian and V. V. Bugayov, Phys. Rev. D **74**, 034018 (2006) [erratum: Phys. Rev. D **79**, 039901 (2009)] doi:10.1103/PhysRevD.74.034018 [arXiv:astro-ph/0606058 [astro-ph]].

[19] M. R. Krumholz, R. M. Crocker, S. Xu, A. Lazarian, M. T. Rosevear and J. Bedwell-Wilson, Mon. Not. Roy. Astron. Soc. **493**, no.2, 2817-2833 (2020) doi:10.1093/mnras/staa493 [arXiv:1911.09774 [astro-ph.HE]].

[20] M. A. Roth, M. R. Krumholz, R. M. Crocker and S. Celli, Nature **597**, no.7876, 341-344 (2021) doi:10.1038/s41586-021-03802-x [arXiv:2109.07598 [astro-ph.HE]].

[21] M. A. Roth, M. R. Krumholz, R. M. Crocker and T. A. Thompson, "CONGRuENTS (COsmic-ray, Neutrino, Gamma-ray and Radio Non-Thermal Spectra). I. A predictive model for galactic non-thermal emission," [arXiv:2212.09428 [astro-ph.HE]].

[22] J. Hinton [SWGO], PoS **ICRC2021**, 023 (2021) doi:10.22323/1.395.0023 [arXiv:2111.13158 [astro-ph.IM]].

[23] A. Albert, R. Alfaro, H. Ashkar, C. Alvarez, J. Alvarez, J. C. Arteaga-Velázquez, H. A. Ayala Solares, R. Arceo, J. A. Bellido and S. BenZvi, *et al.* [arXiv:1902.08429 [astro-ph.HE]].

[24] M. Ackermann *et al.* [Fermi-LAT], Astrophys. J. **799**, 86 (2015) doi:10.1088/0004-637X/799/1/86 [arXiv:1410.3696 [astro-ph.HE]].

[25] F. G. Saturni, C. H. E. .Arcaro, B. .Balmaverde, J. B. González, A. Caccianiga, M. Capalbi, A. .Lamastra, S. Lombardi, F. Lucarelli and R. Alves Batista, *et al.* JHEAp **35**, 91-111 (2022) doi:10.1016/j.jheap.2022.06.004 [arXiv:2208.03176 [astro-ph.HE]].

[26] S. Aiello *et al.* [KM3NeT], Astropart. Phys. **111**, 100-110 (2019) doi:10.1016/j.astropartphys.2019.04.002 [arXiv:1810.08499 [astro-ph.HE]].

[27] A. Ambrosone, W. I. Ibnsalih, A. Marinelli, G. Miele, P. Migliozzi and M. R. Musone, EPJ Web Conf. **280**, 03001 (2023) doi:10.1051/epjconf/202328003001

[28] A. Marinelli *et al.* [KM3NeT], JINST **16**, no.12, C12016 (2021) doi:10.1088/1748-0221/16/12/C12016 [arXiv:2108.00176 [astro-ph.HE]].

[29] W. Idrissi Ibnsalih *et al.* [KM3NeT], PoS **ICRC2021**, 1168 (2021) doi:10.22323/1.395.1168

[30] A. Ambrosone, M. Chianese, D. F. G. Fiorillo, A. Marinelli and G. Miele, EPJ Web Conf. **283**, 04007 (2023) doi:10.1051/epjconf/202328304007